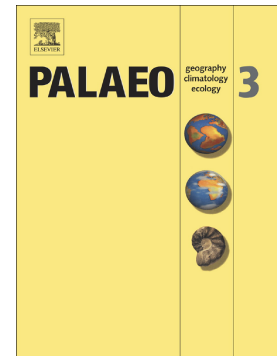


Journal Pre-proof

Middle to late Holocene environmental conditions inferred from paleosols at the perched dune in the Laguna Arturo, Fuegian steppe, southern Argentina

Lorena Laura Musotto, Ana María Borromei, María Soledad Candel, Adriana Mehl, María Virginia Bianchinotti, Andrea Coronato



PII: S0031-0182(21)00591-5

DOI: <https://doi.org/10.1016/j.palaeo.2021.110806>

Reference: PALAEO 110806

To appear in: *Palaeogeography, Palaeoclimatology, Palaeoecology*

Received date: 18 June 2021

Revised date: 15 December 2021

Accepted date: 15 December 2021

Please cite this article as: L.L. Musotto, A.M. Borromei, M.S. Candel, et al., Middle to late Holocene environmental conditions inferred from paleosols at the perched dune in the Laguna Arturo, Fuegian steppe, southern Argentina, *Palaeogeography, Palaeoclimatology, Palaeoecology* (2021), <https://doi.org/10.1016/j.palaeo.2021.110806>

This is a PDF file of an article that has undergone enhancements after acceptance, such as the addition of a cover page and metadata, and formatting for readability, but it is not yet the definitive version of record. This version will undergo additional copyediting, typesetting and review before it is published in its final form, but we are providing this version to give early visibility of the article. Please note that, during the production process, errors may be discovered which could affect the content, and all legal disclaimers that apply to the journal pertain.

Abstract

In the present study, we carried out palynological (pollen, spores, fungal remains, and freshwater algae) and pedological analyses from three paleosols (Ps6, Ps7, and Ps8) that developed in the upper part of the Arturo perched dune deposits, in the periphery of the homonymous lake, and compared the results with modern palynological assemblages from the Fuegian steppe in southern Argentina. These proxies offer an exceptional opportunity to enhance our knowledge of environmental conditions during the Holocene in the southern high latitudes. Pollen spectra from the paleosols Ps6 (middle Holocene), Ps7 and Ps8 (late Holocene) were dominated by Asteraceae subf. Asteroideae undifferentiated, which suggests that herbaceous and/or shrub vegetation probably developed locally on the dune. The existence of herbivorous grazers is indicated by the record of ascospores of several coprophilous fungi (*Coniochaeta* cf. *lignaria*, cf. *Delitschia pachylospora*, cf. *Schizothecium* sp., *Sordaria*-type, *Sporormiella*-type). Most other fungal remains (*Glomus* cf. *Cryptendoxyla hypophloia*, Microthyriaceae, *Alternaria* sp., *Dictyosporium* sp.) are likely associated with the presence of steppe vegetation communities. In general, the paleosols displayed a low degree of pedological development and in one of them (Ps7) there is evidence of the re-activation of eolian processes. Taken together, our palynological and pedological results, as well as sedimentological and geomorphological data, indicate that Ps6 developed under less humid conditions than the overlying paleosols, Ps7 and Ps8. The variations in moisture availability during soil forming intervals could be related to shifts in the latitudinal position and/or strength of westerlies throughout the middle to late Holocene.

Keywords: Pollen. Fungal remains. Paleopedogenesis. Eolian deposits. Paleoclimatic variations. Tierra del Fuego.

1. Introduction

The geographical location of Isla Grande de Tierra del Fuego influenced year-round by the southern westerly winds, makes it a suitable area to study the shifts of these winds in response to changes in the ocean-atmosphere system. In this sense, the northern part of the island, characterized by a relatively homogeneous landscape of extensive plains of grasses and shrubs, offers us the opportunity to investigate climate changes and their effects on semi-arid environments at high latitude.

Late Quaternary vegetation history in the Isla Grande de Tierra del Fuego is mainly known from postglacial pollen data reconstructions from numerous peat bogs and lake sediment cores from the south-central part of the island (Heusser, 2003; Markgraf and Huber, 2010; Borromei et al., 2007, 2010, 2014, 2015; Waldmann et al., 2014; Musotto et al., 2016, 2017a, 2017b, among others). These pollen sequences have shown that most of the area, currently covered by *Nothofagus* forests, was occupied by an impoverished tundra/steppe vegetation with small tree populations after deglaciation, and followed by the development of a forest-steppe ecotone after ca. 11,500 cal yr BP. Forests spread after ca. 7000 cal yr BP because of an increase in the effective moisture of westerly origin. On the other hand, the pollen data from the northern Fuegian steppe also indicated a Late glacial landscape of tundra/steppe vegetation at the Bahía Inútil locality (Heusser et al., 1989-90). During the early Holocene, an almost treeless grass and shrub steppe with shallow, brackish-freshwater bodies developed on the Atlantic coastal areas (Markgraf, 1993; Candel et al., 2020). The Holocene marine transgression, after ca. 8500 cal yr BP, produced an extensive tidal flat on the coastal areas and the development of mainly halophyte vegetation that lasted until ca. 7000 cal yr BP. After that, the grasslands spread over the area surrounding the shallow lake basins during the

middle to late Holocene (Borromei et al., 2018; Candel et al., 2020; Montes et al., 2020).

The Fuegian steppe is characterized by the development of numerous seasonal shallow lakes as pans features (Villarreal and Coronato, 2017). Recently, a paleolimnological record from a lacustrine core obtained from Laguna Arturo (Fig. 1), exposed environmental and climatic oscillations from the Late-glacial onwards (Fernández et al., 2018, 2020a). In addition, the multiproxy data from a lacustrine core from Laguna Carmen (Borromei et al., 2018; Laprida et al., 2021) (Fig. 1B) revealed recurrent dry/wet intervals at centennial- to millennial scale at the Fuegian steppe during the late Holocene. The pans at the Fuegian steppe are located in depressions surrounded by smooth rocky hills covered with eolian deposits in the form of perched dunes. Most of these dunes contain interspersed paleosols (Coronato et al., 2011, 2021) as part of their stratigraphic succession. As is well known, paleosols have been proven to be a valuable source of information about past terrestrial systems in which environmental conditions were imprinted with varying clarity and permanence (Fenwick, 1985). Paleosols also provide evidence on the way vegetation communities and soils responded to paleoclimatic variations (Caseldine and Matthews, 1985). Coronato et al. (2021) described textural patterns of several paleosols interspersed with eolian sediments of perched dunes at the O'Connor, Amalia and Arturo shallow lakes, among others (Fig. 1C), formed since Late-glacial to late Holocene times. In northern Tierra del Fuego, the beginning of a pedologic event about 1000 years ago that affected the upper section of widespread eolian and colluvial deposits was reported (Favier-Dubois, 2003, 2007); the soil is buried in many places by a sandy layer of variable thickness suggesting, according to the author, a further reactivation of morphogenetic processes.

Here we present palynological (pollen, spores, fungal remains, and freshwater algae) and lithological analyses performed on three paleosols interspersed in the upper stratigraphic succession in a perched dune at the Arturo shallow lake, named Ps6, Ps7, and Ps8 paleosols according to Coronato et al. (2011) (Fig. 1), in the northern Tierra del Fuego. Preliminary palynological results have been presented by Musotto et al. (2018). The main goal of this paper is to provide new insights into the middle to late Holocene vegetation and environmental history in the Fuegian steppe related to changes in the climatic conditions. Thus, this study complements existing information about pollen representation from Quaternary deposits in the steppe and adds the modern palynological data for the area of Laguna Arturo. The comparison with other records previously reported will allow us to evaluate the similarities and differences in the environmental changes since the middle Holocene. Of interest is the fungal microbiota identified in the paleosols, as fungal remains are rarely studied in these environments. Two archaeological sites, Arturo 1 and Arturo 2, which are located close to the top of the Arturo perched dune (Fig. 1E), and several isolated archaeological remains spreading along eolian deposits in the lower sectors of the lake coast have been interpreted as different levels of knapping activities (Coronato et al., 2011; Oría and Salemme, 2016; Oría et al., 2016). Therefore, the study of these paleosols also seeks to increase understanding of the Holocene environmental conditions in the Fuegian steppe that could have affected the hunter-gatherer strategies.

2. Climate and vegetation in the Fuegian steppe

Northern Tierra del Fuego is the insular extreme of the Magellanic steppe with a more humid and oceanic climate than the Patagonian steppe. Annual precipitation in the region ranges from 410 mm yr⁻¹ (south of the Río Grande) to 300 mm yr⁻¹ (Cape of

Espíritu Santo, northern tip of Tierra del Fuego) (Fig. 1); precipitation is evenly distributed over the year, decreasing from SW to NE, with a precipitation gradient of 2 mm km⁻¹ in that direction (Quiroga, 2018), as a result of the rain shadow effect of the Andes range (Collantes et al., 1999, 2013). Average temperature is 0.8 °C in July (winter) and 10.1 °C in January (summer) (Quiroga, 2018). Meteorological information is provided by an automatic weather station located at San Julio Ranch, 80 km westwards of the Atlantic coast (Fig. 1C). Winds blow almost constantly, primarily from the west, northwest and southwest (Coronato et al., 2008, 2011). The water balance has a noticeable deficit in summer largely due to the high wind speed that drives high potential evapotranspiration (Collantes et al., 1999). The Aridity Index is 0.75, which is characteristic of the Cold Subhumid Oceanic climate hydric regime that prevails in the region (Coronato et al., 2008).

The composition of the plant communities in the Fuegian steppe is mainly related to the interaction of geomorphology, bedrock lithology, and climate that together determine soil composition and fertility. According to Collantes et al. (1999), two main types of vegetation are observed following a soil nutrient gradient: acidophilous/mesotrophic vegetation in acid soils and neutrophilous vegetation in neutral soils, with four community types in each one (Fig. 1C). The acidophilous types are dominated by *Empetrum rubrum* heathlands and other shrubs (mainly *Chiliodendron diffusum*) and tussocks of *Festuca gracillima*. The neutrophilous vegetation is characterized by predominance of grasses (*F. gracillima*, *Poa* sp.), graminoids (*Carex* sp.), cushion shrubs (*Azorella monantha* and *Azorella trifurcata*), prostate forbs (*Acaena pinnatifida*), and dwarf forbs (*Perezia recurvata*, *Nassauvia darwinii*, and *Colobanthus subulatus*). The valley bottom vegetation ('vegas') is dominated by marshes and meadows.

The main vegetation type in the studied site is the *F. gracillima* tussock grassland with an open community of short grasses and forbs (Posse et al., 2000). It forms a continuous groundcover except where it has been disturbed by overgrazing or human-induced changes (Collantes et al., 1999, 2005).

3. Physical setting at the Arturo Dune

The Arturo Dune is located above a cliff exposed towards the NW, on the southern coast of the homonymous shallow lake ($53^{\circ} 43' 28''$ S; $68^{\circ} 18' 51''$ W; 95 m a.s.l., Fig. 1B and D). According to Coronato et al. (2011, 2021), the landform is a perched dune, that has resulted from the accumulation of short-distance transported sediments, i.e. from the cliff surrounding the lake and from the pan. The cliff is composed of a Middle to Lower Miocene sedimentary sequence made up of silty-clayey sedimentary rocks overlaid by a sandy conglomerate (total thickness: ~15 m); above this, a sequence of 19 m thick eolian deposits had accumulated. The eolian deposit is formed by nine silty loam layers interbedded with eight paleosols that developed on top of each layer. The thicker eolian layer (Eolian 5), contains a 4 cm thick tephra layer (Fig. 2A) related to a Holocene volcanic eruption of Mt. Burney (Coronato et al., 2011), located 400 km north in the Austral Volcanic Zone (Stern, 2008).

4. Methodology

4.1. Sampling, sediment analyses and chronology

The three studied paleosols (Ps6, Ps7 and Ps8) at the Arturo dune were described following the Catt (1990) criteria and sampled during the 2014 southern spring for palynological analysis. Sediment samples of 2 cm thickness were taken at regular intervals, obtaining thirty samples. Additionally, seven surface sediment samples (MS

15–MS 21) were obtained from the Arturo and Carmen lakes area (Fig. 1B) following the multiple sampling method (Adam and Mehringer, 1975); they were added to thirteen previously published surface sediment samples (Musotto et al., 2012), which are also included in the pollen analysis presented here.

Grain-size analysis of paleosols was performed using a Malvern 2000 laser particle size analyzer and results were grouped according to the USDA classification system. Colors in paleosol horizons were determined from air-dried samples through comparison with the Munsell (1973) soil color chart. Both the grain-size and the textural analyses were carried out at the CADIC-CONICET (Centro Austral de Investigaciones Científicas) laboratory (Ushuaia Argentina). The organic matter content data were taken from Coronato et al. (2021), who reported analyses performed by the loss-on-ignition method following Davies (1974) and Page (1982). Nomenclature of buried soils horizons is from Soil Survey Staff (1999).

The obtained chronology is based on six accelerator mass spectrometry (AMS) ^{14}C dates on bulk organic matter sampled from the top and base of each studied palynological section (Table 1). The calibration to calendar years was performed using Calib 8.2 (Stuiver et al., 2021) and the Southern Hemisphere curve (SHCal20) (Hogg et al., 2020). Referring to the age of a paleosol, two concepts need to be considered: the age of the burial and the period of formation that is the elapsed time during which pedogenesis took place (Fenwick, 1985). In this sense, the interpretation of radiocarbon dates based on soil organic matter can be challenging because of soils are open systems characterized by intensive exchange of carbon with the atmosphere and biota in the course of its formation and also with possible inputs and losses of organic matter after burial (McClung de Tapia et al., 2005). Radiocarbon dating of soil organic matter implies the measurement of the mean residence time of various organic fractions

(Walker, 2005), thus radiocarbon ages are generally younger than the true ages of soils (Wang et al., 1996) and those obtained from paleosol humus indicate minimum ages for the pedogenesis processes (Matthews, 1985). In addition, interferences also come from the circulation of humic acids, root penetration, earthworm and other biological activity (Walker, 2005). Hence, radiocarbon ages here presented allowed us to define ‘time windows’ which correspond to intervals of soil formation and landscape stability. These datings were checked against previously published ages by Coronato et al. (2011, 2021). These authors carried out sediment sampling along this dune exposure during 2007-2010 field seasons to determine the dune genesis, the magnetic properties of the eolian sediments, among others. In this study, we focus on a high-resolution palynological record that was obtained from the same dune sedimentary outcrop, but the sampling points were not exactly the same as each other, since the marks left were easily removed due to the intensity of the winds in this region. Therefore, it was not able to fully integrate the available radiocarbon dates from both studies into a paleosol age-depth model.

4.2. Palynological analysis

Surface and fossil sediment palynological samples were sieved through a 150 μm mesh screen and treated with 10% HCl and 70% HF acids in order to remove carbonates and silica, respectively. Two *Lycopodium clavatum* tablets were added to each sample prior to the treatment for the calculation of the palynomorph concentration per gram of dry sediment (Stockmarr, 1971). Finally, the organic residues were sieved through a 10 μm nylon mesh and stained with Safranin-O (Stanley, 1966). Permanent slides were mounted with glycerine-gelatin and examined using transmitted light microscopy (Olympus BX40 and Nikon Eclipse 50i) at 400 and 1000 \times magnification.

Photomicrographs were obtained with AmScope MU 1803 and Olympus C-5060 digital cameras. Modern and fossil palynological slides were stored in the Laboratorio de Palinología at Universidad Nacional del Sur (Bahía Blanca, Argentina) and coded as UNSP followed by the denomination of the sampling site: MS (Muestra Superficial) and PDA (Paleosuelo Duna Arturo).

Due to the low taxonomic resolution of Asteraceae subf. Asteroideae pollen grains that include shrubs and herbaceous genera, they were grouped as Asteraceae subf. Asteroideae undifferentiated (hereafter as Asteroideae undiff.). Dryland taxa plotted were Asteraceae (subfs. Asteroideae undiff., Cichoriaceae, and tribe Nassauvieae), *Berberis*, *Ephedra*, Ericaceae (primarily *Empetrum rubrum*), Chenopodiaceae, Caryophyllaceae, *Acaena*, Rubiaceae, Apiaceae, and *Azorella*. Abundance of *Empetrum rubrum* in the Fuegian steppe is associated to acidic, poor nutrient soils of coarse texture, while in the deciduous forest this taxon is found in association with *Sphagnum* bogs growing on dry hummocks and covering poorly drained lowlands (Moore, 1983). Wetland taxa included *Caltha*, *Cortiana*, *Gunnera*, Ranunculaceae, Urticaceae and *Valeriana*. Cyperaceae, Iridaceae, Juncaceae and *Myriophyllum* were grouped and named as Cyperaceae and other aquatics. Bryophytes and pteridophytes were plotted as spores, and *Pediastrum*, *Botryococcus braunii* and *Zygnema* as freshwater algae.

The frequencies of trees, shrubs, herbs and macrophytes were based on counts between 198 and 496 pollen grains. In modern surface samples, macrophyte frequencies were excluded from the total pollen sum as they represent the local wetland vegetation. Frequencies of spores and freshwater algae were calculated separately and related to the total pollen sum. Fungal remains were also calculated as percentages of the total pollen sum plus fungal remains sum. Plotting of palynological diagrams and statistical analyses was carried out using the TGView 2.6.1 program (Grimm, 2012).

Unconstrained cluster analysis was applied to determine the zonation of the modern samples in the same way as stratigraphically constrained cluster analysis was used to delineate the zonation of the fossil samples. In both analyses Edwards & Cavalli-Sforza's chord distance square-root transformation (CONISS) was used (Grimm, 2012). Pollen types with percentages $\geq 2\%$ were selected for this analysis after recalculating sums and percentages.

Most of the fungal remains (fr) were assigned to modern taxa. Identifying acronyms (Miola, 2012; O'Keefe et al., 2021) were employed to label those fungal remains that have only a superficial morphological resemblance with modern taxa. The fungal specimens assigned identifying acronyms by van Geel and others were indicated as 'HdV-xxx' (HdV = Hugo de Vries- Laboratory, University of Amsterdam, The Netherlands). A systematic list of the fungal taxa is given in the Appendix. Musotto et al. (2012, 2013, 2017b) were consulted as they reported descriptions of some fungal remains found in several types of sediments in Tierra del Fuego.

5. Results

5.1. Paleosol features and chronology

The three paleosols (Ps6, Ps7, and Ps8) buried in the upper section of the eolian deposits of the Arturo Dune show clear and smooth top limits and mostly gradual and smooth bottom limits (Fig. 2). The paleosols have a silt loam texture, silt is the dominant grain size fraction and colors vary between light olive brown (2.5Y5/3) and brown (10YR 5/3). In general, the three paleosols have a relatively low degree of pedological development, but differences among them can be established.

Paleosol 6 (Ps6) is ~50 cm thick, with an A, C profile. It contains 3.2% of organic matter. The A horizon is ~43 cm thick, sandy silt (with a Clay : Silt : Sand grain size

ratio of ~ 18 : 62 : 19) and light olive brown in color (2.5Y 5/3); common bioturbations, resulting in an incipient granular/crumb structure (i.e. peds with a spheroidal or crumb shape); and white mottles up to 2 mm in diameter, likely salts, are observed. The C horizon (~ 20 : 61 : 19) has a similar grain size ratio and color (2.5Y 5/4) to the upper A horizon, with a barely higher (2%) clay content and structureless. The studied palynological interval from Ps6 was radiocarbon dated at 5066 ± 27 ^{14}C yr BP (5799 cal yr BP) and 4424 ± 26 ^{14}C yr BP (4948 cal yr BP) from the base to the top (Table 1).

Paleosol 7 (Ps7) is ~90 cm thick, with a B, A, AC, C profile and sandy silt texture. The organic matter content is 4.86%. The B horizon (~ 18 : 65 : 17), on the top of the paleosol, is 32 cm thick, light olive brown (2.5Y 5/4) in color and presents a weak columnar structure, i.e. the tops of columns are slightly domed; it has clear and smooth upper and lower limits. The A horizon (~ 17 : 63 : 19) is ~32 cm thick and exhibits brown color (10YR 4/3). It is structureless but more compact than lower horizons; the lower limit is transitional. Bioturbation features are abundant and characterized by burrows and channels infilled with fecal pellets. The AC horizon (~ 17 : 62 : 20) is ~ 11 cm thick, structureless, and olive brown in color (2.5Y 4/3); and the C horizon (~ 20 : 51 : 28) is apedal and olive brown in color (2.5Y 5/3). From the base to the top of the studied palynological interval, the radiocarbon dates indicated an age of 2902 ± 24 ^{14}C yr BP (2987 cal yr BP) and of 1752 ± 22 ^{14}C yr BP (1620 cal yr BP) (Table 1).

Paleosol 8 (Ps8) is nearly 50 cm thick and presents an A, AC, C profile, with transitional limits between horizons and slight differences in grain sizes. The organic matter content is 4.87%. The A horizon is 19 cm thick, primarily sandy silt (~ 17 : 66 : 17), structureless, light olive brown (2.5Y 5/3) in color, and exhibits a weak granular structure. The AC horizon is sandy silt (~ 18 : 64 : 18) and brown (10YR 5/3) in color while the C horizon, ~ 20 : 51 : 28, is light olive brown (2.5Y 5/3); both the AC and C

horizons are structureless. The studied palynological interval from Ps8 was dated at 2406 ± 52 ^{14}C yr BP (2415 cal yr BP) and 1538 ± 41 (1377 cal yr BP) from the base to the top (Table 1).

When comparing the three paleosols, Ps7 has the highest degree of pedological development while Ps8 has a slightly more conspicuous degree of horizonation than Ps6. The paleosols do not exhibit significant differences related to clay content and illuviation processes; clay : silt ratio in Ps6 (0.31 average) is barely higher than in Ps7 (0.27 average) and Ps8 (0.26 average).

5.2. Modern pollen and fungal assemblages

In the modern pollen diagram (Fig. 3) the forest communities are represented when *Nothofagus dombeyi*-type frequencies are higher than 50% and Poaceae lower than 20%. On the other hand, the steppe is characterized by Poaceae pollen values that range between 16% and 65% and *Nothofagus* less than 35%; while the transitional ecotone between forest and steppe is denoted by *Nothofagus* frequencies up to 50% and Poaceae up to 20%.

The unconstrained cluster analysis of the pollen record from the steppe surface samples (Fig. 1B) allowed to define permitted differentiation of three palynological groups designated S1, S2 and S3 (Fig. 3; Table 2). The samples grouped in S1 and S2 have low percentages of Poaceae (16–37%), while in the S3 samples Poaceae records the highest values (40–65%). Asteraceae subf. Cichorioideae reaches up to 24% and Asteroideae undiff. registers 19–23% in samples grouped in the S2 type. The S1 type steppe records the highest proportions of *Azorella* (up to 58%). Other herbs (*Acaena*, Apiaceae, Brassicaceae, Caryophyllaceae, Chenopodiaceae, *Gunnera*, *Rumex acetosella*) are also present with low frequencies (<5%) in the three palynological types.

In particular, it is observed that the *Nothofagus dombeyi*-type pollen exhibits the highest frequency value (38%) in sample MS 15, while in the other steppe surface samples, its frequencies do not surpass 33%.

With regard to fungal spores, *Glomus* appears with low percentage values (<6%) in the samples grouped as S1, while it reaches its highest frequencies (up to 72%) in most of the S2 group samples. Ascospores of *Sporormiella*-type (<24%) and *Sordaria*-type (<11%) are present in the three steppe types, while reproductive bodies of Microthyriaceae are found in low frequencies (<1%). Ascomata of cf. *Cryptendoxyla hypophloia* (<1%) are restricted to the S2 steppe samples. Spores of *Arthrinium puccinioides* and *Dictyosporium* sp. register percentages of <1% in the three steppe types, while *Tetraploa aristata* (<2%) is only recorded in few samples of the S2 and S3 steppes.

5.3. Fossil pollen and fungal assemblages

5.3.1. Paleosol 6

The palynological record from Ps6 is divided into two palynological zones (Ps6-1 and Ps6-2; Fig. 4).

Zone Ps6-1 (22–13 cm) is dominated by Asteroideae undiff. (40-52%) accompanied by Caryophyllaceae (up to 13%). Asteraceae subf. Cichorioideae (7%), Poaceae (6%) and *Acaena* (<4%) are also present. Other taxa (i.e. Brassicaceae, *Valeriana*, Ericaceae, and Chenopodiaceae) show low proportions (<1%). *Nothofagus dombeyi*-type, the arboreal component, ranges between 21 and 30%. Low frequencies of macrophytes, Iridaceae (<6%) and freshwater algae (<3%) are recorded. *Glomus* fluctuates between 7 and 12% while *Sordaria*-type reaches up to 5%. Other fungal taxa (cf. *Schizothecium* sp., cf. *Acaulospora* sp., and conidia of *Alternaria*) are present with

low values (<1%). Total pollen concentration reaches 610 grains g^{-1} and total fungal concentration displays very low concentration values (90 fr g^{-1}).

In Zone Ps6-2 (13–0 cm) Asteroideae undiff. decreases from 45% to 35% and Caryophyllaceae attains similar values (<12%) as in the previous zone. *Acaena* (<6%) and Asteraceae subf. Cichorioideae (<4%) are also present, while Poaceae declines to 2%. *Nothofagus dombeyi*-type increases and ranges between 36 and 40%. Iridaceae (3%) and freshwater algae (4%) remain in low percentages. *Glomus* spores record up to 13% at the beginning of this zone, followed by a decline towards the top (8%); while *Sordaria*-type (5%) shows similar values as in the previous zone (Ps6-1). Total pollen concentration increases up to 735 grains g^{-1} and total fungal concentration up to 125 fr g^{-1} .

5.3.2. Paleosol 7

Three palynological zones (Ps7-1 to Ps7-3) were identified in the record from Ps7 (Fig. 5)

Zone Ps7-1 (57–43 cm) is characterized by high Asteroideae undiff. percentage values (47–65%). Poaceae (<8%), Asteraceae subf. Cichorioideae (<3%) and Caryophyllaceae (<5%) show low values. *Nothofagus dombeyi*-type is present with 36% and decreases to 27% towards the end of the zone. Macrophytes, primarily represented by Cyperaceae, record up to 5%. Among the fungal remains, *Glomus* increases from 69 to 77%. Meanwhile, spores of cf. *Schizothecium* sp., *Sordaria*-type, cf. *Acaulospora* sp., Type HdV-181 and ascomata of cf. *Cryptendoxyla hypophloia* are present with low values (<2%). Total pollen concentration values reach 2300 grains g^{-1} and total fungal concentration registers 8700 fr g^{-1} .

In Zone Ps7-2 (43–23 cm) Asteroideae undiff. (78%) increases and attains the maximum frequencies throughout this record. Poaceae (2%) maintains similar values than the previous zone (Ps7-1). Other taxa (Asteraceae subf. Cichorioideae, Caryophyllaceae, Apiaceae, and Ericaceae) are present with low values (<2%). *Nothofagus dombeyi*-type drops to <17%. Macrophytes decline to <1%. *Glomus* spores increase and fluctuate between 74 and 84%. Total pollen concentrations range between 2900 and 4900 grains g⁻¹ and total fungal concentrations increase up to 22,800 fr g⁻¹.

In Zone Ps7-3 (23–0 cm) Asteroideae undiff. declines to 54% at the beginning of the zone and then rises to 62%. Poaceae (4%), Asteraceae subf. Cichorioideae (5%), and Caryophyllaceae (2%) increase slightly. *Acaena*, Apiaceae and Brassicaceae are present with low values (<2%). *Nothofagus dombeyi*-type increases up to 33% in the lowermost part of the zone and afterwards decreases to 21%. Iridaceae and Cyperaceae are present (<5%). *Glomus* declines from 86% to 67% and then increases up to 82% at the end of the zone. Ascospores of cf. *Schizobolus* sp., *Sporormiella*-type and *Sordaria*-type record low (<2%) proportions. Other fungal taxa (cf. *Acaulospora* sp. and *Dictyosporium* sp.) are also present. Total pollen concentration records a maximum of 6400 grains g⁻¹ and then declines to 3200 grains g⁻¹. The concentration of fungal microfossils remains high (21,500 fr g⁻¹) and achieves a maximum of 30,500 fr g⁻¹ in the middle of this uppermost zone.

5.3.3. *Paleosol 8*

The palynological record from Ps8 is divided into three palynological zones (Ps8-1 to Ps8-3; Fig. 6).

In Zone Ps8-1 (52–38 cm) Asteroideae undiff. increases from 34% to 52% followed by a decrease (38%) towards the end of the zone. Poaceae is present in low (<7%)

values. Herbaceous taxa (*Acaena*, Caryophyllaceae and Rubiaceae) and Chenopodiaceae show low (<6%) proportions. *Nothofagus dombeyi*-type reaches values up to 45%. Cyperaceae is present in low frequencies (4%). Fungal assemblage is dominated by coprophilous spores of cf. *Schizothecium* sp. (11%) and Sordariales s.l. (11%) accompanied by *Sordaria*-type (4%), cf. *Delitschia* sp. (3%) and *Sporormiella*-type (3%). Dematiaceous spores of *Dictyosporium* sp. show low (2%) proportions at the top of the zone. Total pollen concentration records 2000 grains g⁻¹ and fungal remains concentration fluctuates between 300 and 700 fr g⁻¹.

Zone Ps8-2 (38–8 cm) is divided into two subzones. In subzone Ps8-2a (38–28 cm) Asteroideae undiff. increases up to 51%, while Poaceae declines to 4%. *Acaena*, Caryophyllaceae, Brassicaceae and Asteraceae subf. Cichorioideae are present with low values (<2%). *Nothofagus dombeyi*-type decreases to 36% at the end of the subzone. The macrophytes record low (>2%) percentages throughout the paleosol profile. Fresh-water algae (mainly *Botryococcus braunii*) increase up to 2%. Ascospores of cf. *Schizothecium* sp. (5%) and *Sordaria*-type (1%) show the lowest proportions of the entire record. *Sporormiella*-type reaches up to 2%. Other fungal taxa include cf. *Delitschia pachylospora*, *Glomus*, cf. *Acaulospora* sp., and cf. *Cryptendoxyla hypophloia*. Total pollen concentration (1800 grains g⁻¹) maintains similar values relative to the previous subzone (Ps8-1), while fungal concentrations decline to <180 fr g⁻¹.

In subzone Ps8-2b (28–8 cm), Asteroideae undiff. (46%) shows similar percentages to those in subzone Ps8-2a. Poaceae (5%) slightly increases. *Acaena*, Caryophyllaceae, Rubiaceae, Brassicaceae, and *Valeriana* are present with low values (<1%). *Nothofagus dombeyi*-type ranges between 36 and 43% throughout the subzone. Fungal ascospores of cf. *Schizothecium* sp. decrease from 8% to 4% towards the end of the subzone.

Sordaria-type reaches up to 6%, while cf. *Delitschia* sp. and cf. *Delitschia pachylospora* appear with low frequencies (2%). Ascomata of cf. *Cryptendoxyla hypophloia* (<2%) and spores of *Dictyosporium* sp. (<4%) are also present. Total pollen concentrations reach up to 2400 grains g^{-1} and total fungal concentrations vary between 200 and 700 fr g^{-1} .

Zone Ps8-3 (8–0 cm) displays an increase in Asteroideae undiff. (48-52%). Poaceae (6%) maintains similar values than the previous subzone (Ps8-2b), while *Acaena* and Asteraceae (tribe Nassauvieae) increase to 4% and 2% respectively. Other herbs (Caryophyllaceae, Rubiaceae, Brassicaceae and *Valeriana*) are present with low values (<2%). *Nothofagus dombeyi*-type decreases from 32% to 29% towards the end of the zone. Among fungi, cf. *Delitschia* sp., cf. *Schizothecium* sp. and *Sordaria*-type increase up to 6% at the top of the zone. Other taxa include *Glomus* (7%), cf. *Acaulospora* sp. (<2%), Microthyriaceae (1%), and *Dictyosporium* sp. (5%). Total pollen concentrations increase up to 3200 grains g^{-1} and total fungal concentrations up to 1200 fr g^{-1} .

6. Discussion

6.1. Interpretation of modern pollen and fungal assemblages

The modern pollen assemblages (Fig. 3) reflect the three major vegetation units recognized in Tierra del Fuego, that, by and large, follow a southwest to northeast climatic and topographic gradient. Thus, at regional scale, *Nothofagus dombeyi*-type and Poaceae are the taxa that characterize the main vegetation units, i.e. the forest and the steppe, respectively. In particular, factors such as the structure of the landscape, edaphic characteristics and land use (e.g. grazing), are relevant to model the ecosystem and vegetation dynamics in the Fuegian steppe (Paruelo et al., 1998). The modern pollen data show that samples from S1 and S2 steppe groups, characterized by low

percentages of Poaceae, probably indicate the effect of grazing on the grassland communities. While in the S3 samples group, Poaceae proportions (40-65%) indicate a lower grazing effect than in S1 and S2, and correlate well with the steppe surface samples reported by other authors (Heusser, 1989; Trivi de Mandri et al., 2006). In the S1 steppe, peak amounts of *Azorella* indicate severe mechanical damage caused by livestock trampling and soil compaction. After the arrival of Europeans cattle settlers, at the end of 19th century, sheep overgrazing led to the encroachment of non-palatable plants, especially *Azorella trifurcata*, which has a prostrate growth form, thus making it resistant to trampling (Posse et al., 2000; Collantes et al., 2013). Additionally, it is likely that the long roots of *Azorella* increase the water uptake, lowering the water table and making it less available for grasses and other herbaceous vegetation (Collantes et al., 2013). The grazing effect can also be demonstrated by the relative preponderance of Asteraceae subfs. Asteroideae undiff. and Cichorioideae in the S2 steppe samples. Asteraceae includes forbs with grazing response characteristics, such as rosette growth forms, which are more tolerant to trampling compared to erect forms of forbs, shrubs and grasses (Posse et al., 2000). Asteraceae subf. Cichorioideae would be most likely represented by the invasive exotic weed *Hieracium pilosella*, first detected and reported in 1993 (Rauber, 2011). Its introduction and expansion in the Fuegian steppe was likely promoted by selective-feeding grazing, trampling, and increasing seed dispersal by herbivores (Cipriotti et al., 2014). The high proportion of *N. dombeyi*-type, an extra-regional taxon, in sample MS 15 is likely the result of low local pollen production that leads to over-representation of distant taxa in the percentage diagram, which gives a false impression of the vegetation abundance (Birks and Birks, 1980).

Among fungal remains, *Glomus* spp. are the most common arbuscular mycorrhizal fungi (AMF) (Smith and Read, 2008) and their chlamydospores are recorded only in the

steppe surface samples (Fig. 3). Spores of several AMF species occur in rhizospheric soils around the most frequent grasses in grasslands degraded by sheep grazing in Tierra del Fuego (Mendoza et al., 2011). The effect sheep grazing exerts on AMF colonization is often controversial. According to Cavagnaro et al. (2019), the process, which includes mechanical disturbance such as damage by trampling and physical erosion, could break down the hyphal network with the consequent reduction in root colonization by these fungi. Therefore, the low percentages of *Glomus* recorded in the S1 samples might be suggesting that the mycorrhizal colonization was probably reduced by intense grazing conditions. However, in some circumstances defoliation may have no effect, or even increase the degree of colonization by AMF. It is possible that where herbivory is exerted in low to moderate levels it could be beneficial to establish plant–microbial interactions through enhanced root exudation (Wearn and Gange, 2007) as indicated by the highest frequencies of *Glomus* in most of the S2 samples from grazing sites. On the other hand, cephalothecoid peridium remains belonging to cf. *Cryptendoxyla hypophloia* are present in these samples. This fungus has a saprophytic lifestyle, with great affinity for cellulose-rich substrates, like very rotten wood (Greif and Currah, 2007). The almost continuous record of remains of ascomata or ascospores from *Sporormiella*-type and *Sordaria*-type in all the surface samples, suggests the presence of herbivorous grazers in the environment, but whether these are native grazers (like *Lama guanicoe* ‘guanaco’ or *Ctenomys magellanicus* ‘tuco-tuco’) or domesticated animals (sheep and cows) cannot be resolved. Both fungal genera are representative of coprophilous growth habits, characterized by spores that are ingested by herbivores while feeding, that survive digestion and then germinate in the dung (Baker et al., 2013). *Tetraploa aristata*, a species often recorded on senescent culms of Poaceae and Cyperaceae is a major saprophytic fungus (Tanaka et al., 2009) also present in the

steppe samples dominated by grassland communities. Microthyriaceae reproductive bodies are mostly found in the forest, though they are also present in the steppe communities, suggesting locally humid environments. Microthyriaceae are epiphyllous fungi and their occurrence is dependent on the availability of humid conditions (García Massini et al., 2004). Spores of *Dictyosporium* sp. are also recorded in the forest and in the three steppe types (S1, S2, and S3) (Fig. 3). These dematiaceous spores occur in plant debris, soil, wood and wood submerged in freshwater (Sánchez, 2011). The record of spores of *Arthrimum puccinioides* is likely related to the presence of sedges growing close to Laguna Arturo. This fungus usually grows on dead leaves of various species of Cyperaceae (Saccardo, 1886; Ellis, 1971) in Tierra del Fuego environments (Ellis, 1971).

6.2. Palaeoenvironmental and palaeoclimatic reconstruction of the paleosols at Arturo dune

The pollen records identified at the buried soils Ps6, Ps7 and Ps8 (Figs. 4–6) show the dominance of herbaceous/shrubby communities (Asteroideae undiff.) with low proportions of grasses (Poaceae) and herbs (Caryophyllaceae, Asteraceae subf. Cichorioideae, *Acaena*, Brassicaceae, Rubiaceae, *Valeriana*) during the middle to late Holocene. According to Frazer et al. (2020), Asteraceae pollen types have a rapid deposition rate and could be deposited by gravity on a local scale. Thus, local past vegetation also could have comprised scrublands of *Chilotrimum diffusum* ('mata negra') associated with perennial herbs since they develop nowadays on the slopes of the hills and glaciofluvial terraces of the semi-arid steppe (Collantes et al., 1987). These fossil pollen assemblages cannot be easily matched with our modern steppe analogues because of human impact (sheep grazing, livestock activities, invasive species

introduction, among others) that has altered the native vegetation, and likely the way it is represented in the pollen assemblages. Noticeable is the low frequency values of Poaceae recorded in the fossil samples, which could be the result both from the taphonomic processes (e.g. differential pollen preservation), and from unsuitable environmental conditions for the growth of tussock communities over the dune. In this sense, *Festuca gracillima*, the dominant tussock grass in the region, does not seem to tolerate waterlogging conditions, fine-textured soils, or moderate or high salinity or alkalinity (Oliva, 1996). These sediment characteristics are dominant in the Arturo dune where a moderate alkalinity has been inferred based on the pedological structure at the top of Ps7 (B horizon). The pH values on the three paleosols, measured in a soil : water (1:1) method, ranged from 7.75 to 8.53, but these values could be influenced by diagenetic processes and other factors (e.g. parent material composition) according to Lukens et al. (2018). Taken together, the predominance of local herbaceous/shrubby vegetation (Asteroideae undiff.) would be masking the regional pollen signal represented by grassland paleocommunities during the middle to late Holocene (Borromei et al., 2018). Additionally, the paleodune morphodynamic, such as sedimentary accumulation, either preventing or delaying the growth of grasses by burying with eolian sediment would have affected the type of vegetation associations, the species cover and its distribution.

The record of halophytes (Chenopodiaceae) is linked to the vegetation surrounding the shallow Arturo lake, while freshwater algae (*Botryococcus braunii* and *Pediastrum*) likely originate by deflation from the lacustrine dry bottom sediments (Fig. 1D).

The fungal assemblages found in the three paleosols included representatives of Glomeromycota (AMF) (Figs. 4–6). AMF facilitate plant recruitment and growth by mitigating environmental stresses, e.g. nutrient and water deficiencies (Smith and Read,

2008). Chlamydozoospores are formed below the soil surface and normally not transported (Almeida-Lenero et al., 2005). Unfortunately, there are no available studies of the mycorrhizal colonization in Asteraceae roots from the Fuegian steppe, but the high occurrence of *Glomus* spores would suggest a potential association with this family.

The obtained radiocarbon ages from Ps6, Ps7 and Ps8 (Table 1) fit well with those ages from the same pedologic units previously published by Coronato et al. (2021). However, few inconsistencies between dates on bulk organic matter are observed. An example of this is our obtained basal age from Ps8 (2406 ± 52 ^{14}C yr BP, Table 1), which is 1150 radiocarbon years younger than that reported by Coronato et al. (2021). Another case is Ps6, which provided a basal age of 5055 ± 27 ^{14}C yr BP (Table 1), that is an older age than that published by those authors. This inconsistency of dates might be explained because the sampled sedimentary sections were not exactly at the same points, centrimetric lateral variations may have occurred in the buried soils, e.g. topography of the surface at the soil formation interval. Radiocarbon dating performed on faunal remains has also yielded ages unlike those obtained in bulk organic matter. The date on a *Lama guanicoe* bone remains in Ps7 (434 ± 43 ^{14}C yr BP; Coronato et al., 2011) rejuvenated the chrono-stratigraphic sequence. Coronato et al. (2021) reported a new bulk soil organic matter dating that adjusts well to the date here obtained for the basal part of Ps7, discarding the bone radiocarbon date.

On the other hand, the apparent contemporaneity of Ps7 and Ps8 (Table 1) would be related to a variety of factors. Bioturbation is a natural process occurring in paleosols and conducting a vertical mixing of sediments and sedimentary organic matter on the soil/paleosol profile (Kristensen et al., 2012; Hoang et al., 2018). Particularly Ps7 exhibits abundant bioturbation related to faunal activity in the identified A horizon. Besides, the studied paleosols are interspersed in the deposits of an eolian dune

exhibiting several episodes of eolian reactivation. Geomorphological processes such as erosion, reworking, and redeposition of the own dune sediments can incorporate older sedimentary organic matter in younger soils/paleosols and could lead to mistaken chronological interpretations (Coronato et al., 2021). Taking into account that paleosol horizons are overlain by a relatively thin sediment cover, the action of the subsequent root system stabilizing the eolian cover cannot be discarded as it increases the likelihood of contamination of the soil organic content. In spite of this, the general chronological framework of the succession of paleosols recorded at the Arturo Dune is consistent as reported by Coronato et al. (2021).

Paleosol Ps6 exhibits a poor development (5800–4900 cal yr BP), with an A horizon with incipient granular/crumb structure and common bioturbation. The presence of dryland taxa, i.e. Caryophyllaceae (probably *Colobanthus*-type) and *Acaena* pollen (Fig. 4), characteristic of arid environments of the Fuegian steppe (Cingolani, 1999; Mansilla et al., 2018), allow us to infer less humid conditions than Ps7 and Ps8. Preserved pedological characteristics could indicate a less airy and less permeable soil than Ps7, which exhibits a E, A, AC, C with a columnar B horizon on top and a lower A horizon with abundant bioturbations. As regards organic matter content, Ps6 records the lowest content of the three analyzed paleosols. In this sense, the stabilizing effect of organic matter in soils depends strongly on the amount of incorporated organic matter into the uppermost horizons (i.e. at a low incorporation of organic matter, there is a lower stabilizing effect of vegetation) and/or the degree of organic matter decomposition / preservation (Hartge et al., 1994). The low total pollen concentration registered in this paleosol could reflect a low input of pollen grains to the soil, and consequently, a scarce vegetation cover and/or unfavorable taphonomic conditions for the preservation of the pollen grains (Campbell, 1999). The organic matter content

(3.2%, Coronato et al., 2021) and the white mottled features observed could be indicators of low moisture availability and/or high evapotranspiration. Together, they could have contributed to limit fungal activity, which otherwise would have degraded the plant material. In this section, few fungal remains were recorded, with low diversity. One of the fungi recovered was *Alternaria*, in low abundances. *Alternaria* species are widespread, some as saprobic opportunists, endophytes or pathogens, mainly of plants; they can be found on many kinds of substrates, and their spores are mainly wind dispersed (De Linares et al., 2010; Woudenberg et al., 2013).

Paleosols Ps7 (3000-1600 cal yr BP) and Ps8 (2400-1400 cal yr BP) showed a slightly higher degree of pedological development and an increase in the organic matter content (4.86 and 4.87%, respectively; Coronato et al., 2021) and in the pollen and fungal taxa than Ps6. These characteristics likely implied more effective humidity and mild climatic conditions during the soil forming intervals recorded through a higher input of organic matter to upper horizons of both paleosols and more abundant bioturbations at A horizon in Ps7. This is in line with the significantly increasing pollen and fungal concentration values registered in both paleosols. Dematiaceous spores of *Dictyosporium* sp. identified in the Ps7 and Ps8 are in agreement with a major accumulation of organic matter during paleosols development and more humid conditions. The regular presence of Microthyriaceae in the fungal assemblages reflects similar conditions, which are considered essential for its rapid spread (Limaye et al., 2007). Additionally, saprophytic fungi as cf. *Cryptendoxyla hypophloia* are indicative of the presence of decaying wood and good humidity in the ground (Greif and Currah, 2007). The increasing frequencies of *Glomus* spores observed in the Ps7 could be related to a longer pedological interval as indicated by obtained dates and paleosol features, and/or more stable environmental conditions than in Ps6 and Ps8.

The record of ascospores of coprophilous fungi primarily in the Ps7 and Ps8 suggests the local presence of native herbivores in the surroundings of Laguna Arturo. Similar fungal spores have been reported in modern feces of guanaco collected from dung piles located in the Perito Moreno National Park (47° S; 72° W) (Velázquez and Burry, 2012). Coronato et al. (2011) reported a faunal assemblage represented by bones of *L. guanicoe* and *Ctenomys* sp., recorded both in the eolian deposits of the Arturo dune and most of the paleosols interspersed in this dune succession.

The paleosol Ps7 shows an B horizon burying a previously developed soil profile (A, AC, C), which is indicative of a two-stages of soil development. It is interpreted as a reactivation of eolian processes; it would have been a brief lapse featured by the accumulation of ~32 cm thick eolian deposit subsequently experimenting pedogenesis and likely resulting in the formation of A-B paleosol profile with an A horizon then eroded by reactivation of eolian activity. The columnar structure observed in B horizon is a feature commonly found in sodic soils, condition that could be related to differential distribution of exchangeable Na⁺ (due to overland-flow, throughflow and groundwater fluctuations in semiarid climatic conditions (Schaefer and Dalrymple, 1996) and/or subsequent diagenesis. In this case, B columnar structure is weak, and could indicate an incipient soil alkalization without clay enrichment in lower soil horizons suggesting a Na⁺ input from eolian dust coming from the Arturo lake lacustrine bed during desiccation intervals and/or from the Middle to Lower Miocene deposits forming the cliff. Near the study area, Crosta et al. (2014) identified halite crystals in Laguna Escondida (Fig 1C) as a result of precipitation of salts during times with a deficit hydric balance. Also, the dry bottom sediments of Laguna O'Connor and the eolian mantles in the leeward of Laguna Escondida (Fig 1C) contain high values of sodium (Villarreal et al., 2014).

8. Regional inferences

In the Fuegian steppe, the eolian dunes with interspersed paleosols located in the surroundings of Laguna Arturo, Laguna O'Connor and Laguna Amalia (Fig. 1C), among others, have been interpreted as the result of a high climatic variability during the late Pleistocene-Holocene times (Coronato et al., 2021). According to these authors, the alternation of eolian deposits and paleosols indicated the occurrence of arid periods with intense eolian activity followed by more stable environmental conditions which favored the pedogenesis in the topmost parts of the eolian layers. Proxy data obtained from sedimentary cores at Laguna Arturo (Fernández et al., 2020a) and Laguna Carmen (Borromei et al., 2018; Laprida et al., 2021) showed changes in their hydrological conditions suggesting cyclic dry/wet intervals during the Holocene. This has been associated not only to climate events of local occurrence but also to regional climate changes linked to variations in strength and/or latitudinal position of the westerly winds.

Despite the uncertainties of temporal resolution and limited radiocarbon control, our present study contributes to the understanding of regional climate change. The environmental magnetism studies in the Arturo dune suggested that the moisture conditions differed for each paleosol (Orgeira et al., 2012). The magnetic parameters showed a period of higher humidity than the present in the Ps7; while lower water storage is suggested during formation of Ps6. Our palynological and pedological data from Ps6 reflected less humid conditions during the middle Holocene than those from Ps7 and Ps8, during the late Holocene. Arid conditions have also been inferred in the Laguna Arturo sedimentary core during this time. The diatom and ostracod assemblages identified in this record evidenced the presence of a very shallow lake with a negative hydrological balance indicative of ephemeral environments around 6200 cal yr BP

(Fernández et al., 2020a). At Laguna Las Vueltas, located ca. 20 km to the northeast of the study site and on the Atlantic coast (Fig. 1C), there was a regressive phase with the development of a shallow lake disconnected from the sea after ca. 7000 cal yr BP. Meanwhile, changes in the algae content and geochemistry of the lake indicated abrupt events of desiccation and flooding (Candel et al., 2020). Westwards, the pollen data from Lago Lynch (Fig. 1A) showed an increase in effective moisture after ca. 6750 cal yr BP with the increase of *Nothofagus* forest (Mansilla et al., 2018). According to Garreaud et al. (2013), an intensification of westerlies would be linked to a marked west-east precipitation gradient that would result in arid and evaporative conditions over the steppe.

During the late Holocene, the development of the Ps7 and Ps8 pointed to relatively more humid conditions than the Ps6, as it can be inferred mainly by the fungal microfossils indicative of effective soil moisture, and the increase in the organic matter content. These environmental conditions may have favored the presence of hunter-gatherer groups in the area (Oría, 2014). In particular, Laguna Arturo constitutes an archaeological site of interest since it has been considered a meeting point for humans and wildlife in the past (Coronato et al., 2011; Oría et al., 2016; Fernández et al., 2018). The guanaco was a terrestrial staple providing food and raw materials of various types (skins, bones, and tendons, among others) for hunter-gatherers (Fernández et al., 2020b). Evidence of human occupation in Arturo 1 archaeological site has so far been confined to the upper part (Ps7 and Ps8) of the dune depositional sequence and was interpreted as an occasional hunting–primary butchering camp (Coronato et al., 2011, 2021). This could be related with the intervals of wetter conditions observed in Laguna Carmen during the late Holocene (Borrromei et al., 2018; Laprida et al., 2021). Also, at Laguna Potrok Aike (51° S; 69° W) located northwards, in the semi-arid Patagonian

steppe, the pollen data indicated an increase in the moisture availability after 2300 cal yr BP (Wille et al., 2007). The development of Ps7 and Ps8 was, in general, contemporary with a period of reduced humidity reported from western Andean regions between 4000 and 2000 cal yr BP and related to a weakening of westerlies (Mansilla et al., 2016; Echeverría et al., 2017). At present, precipitation events in the semi-arid steppe tend to be slightly larger under weak westerlies or even easterly flows and advection of moisture from the Atlantic (Berman et al., 2012; Garreaud et al., 2013).

In particular, the pedological features observed in Ps₇ are indicative of two episodes of soil formation, most likely due to a re-activation of the eolian processes interrupting pedogenesis. Evidence of intense eolian activity has been mentioned in some localities near the study site. At Laguna Las Vueltas, the sedimentary record revealed arid environmental conditions with an increased deflation activity together with the development of lunette dunes during the late Holocene (Candel et al., 2020; Montes et al., 2020). Traces of long-distance *Drimys winteri* pollen were reported at Laguna Carmen and Laguna Las Vueltas during this time, suggesting periods of stronger-than-present westerlies with a drying effect in the area (Borromei et al., 2018; Candel et al., 2020). This arboreal taxon grows in the west/southwest of Tierra del Fuego along the outer coastal area and produces large, heavy pollen grains which are released as tetrads with limited dispersal capability (Vilanova et al., 2019). Further north, Laguna Azul (52° S; 69° W) documented an increase in the *Nothofagus* pollen amounts indicative of stronger aridity related to an intensification of the westerlies reaching its full strength in the southeastern Patagonia around 3000 cal yr BP (Zolitschka et al., 2019). Conversely, in the Laguna Arturo sedimentary core, the diatom assemblages did not reflect any hydrological change during the late Holocene (Fernández et al., 2020a). Probably, it would be related to the differential response and

susceptibility of each proxy to climate change or to even short-term changes or occasional climate events (Kilian and Lamy, 2012).

Concerning the long-distance *Nothofagus* pollen, the frequency values (up to 45%) recorded in the three paleosols correlate well with those from Laguna Carmen and Laguna Las Vueltas sites (Borromei et al., 2018; Candel et al., 2020). Comparing these values with those from our steppe surface samples, we argue that the forest-steppe boundary was probably not so far from the studied site. The fluctuating *Nothofagus* pollen frequencies observed mainly in Ps7 and Ps8, may be related to intensification/weakening of the westerlies. Although more benign climatic conditions are inferred during the paleosol forming intervals, the rise in the extra-local *Nothofagus* pollen could be indicative of increased winds in the area. During the windy periods, the deep west-east precipitation gradient results in highly evaporative conditions over the Fuegian steppe (Garreaud et al., 2013), affecting directly the water content in the shallow lakes and the development of local vegetation, and leading to more arid palaeoenvironmental conditions.

9. Conclusions

The present contribution constitutes a new approach by combining pollen, fungal and pedological analyses performed on paleosols Ps6, Ps7 and Ps8, buried in the upper section of the Arturo perched dune, in the Fuegian steppe. This offered an exceptional opportunity to reconstruct about the vegetation and environmental conditions that prevailed during pedogenetic processes intervals since middle to late Holocene. The pollen assemblages recorded in these paleosols showed the presence of local shrubby/herbaceous paleocommunities of Asteroideae undiff., which could be attributed to their adaptation to the geomorphological dynamic of the dune. These plant

assemblages differ from the present ones, in which caespitose grasses, forbs and cushion-type vegetation dominate on the Arturo dune. In this sense, our modern palynological datasets reflected the effects caused by human activities and did not provide accurate analogues to interpret the fossil records.

The development of these paleosols was associated with relative landscape stability, favorable to pedogenesis and better climate conditions in the Fuegian steppe, coincident with periods of less aridity and wind than today. Pedological features of the paleosols indicate that these are weak to moderately developed, with reactivation of the eolian erosion in Ps7. While the Ps6 showed a weak horizonation, pollen taxa and scarce fungal remains revealed that this paleosol evolved under arid and windy environmental conditions probably as a result of the intensification of westerlies during the middle Holocene. Conversely, the more humid conditions recorded in the Ps7 and Ps8 were most likely related to a weakening of westerlies and/or even easterly flow and advection of moisture from the Atlantic, during the late Holocene. At present, the dryness or humidity in the region are regulated by the interplay of air masses from the South Pacific and southern seas air masses, which lose their humidity when cross several mountain barriers of the Fuegian Andes reaching the steppe as dry winds, or from the Atlantic Ocean air masses flowing without topographic obstacles. These present conditions would have been accentuated during the middle to late Holocene forcing cycles of eolian deposit-pedogenesis in the Fuegian steppe which proves the alternance of humid and dry atmospheric conditions in lapses shorter than a millennium.

Appendix. Fungal taxa list.

Phylum GLOMEROMYCOTA C. Walker & A. Schüßler, 2001

cf. *Acaulospora* sp. (Figure 7, 19)

Glomus sp. (Type HdV-1103) (Figure 7, 18)

Phylum ASCOMYCOTA Cavalier-Smith, 1998

Cercophora-type (Type HdV-112) (Figure 7, 7)

Coniochaeta cf. *lignaria* (Type HdV-172) (Figure 7, 2)

cf. *Cryptendoxyla hypophloia* Malloch & Cain, 1970 (Figure 7, 22)

cf. *Delitschia pachylospora* Luck-Allen & Cain, 1975 (Figure 7, 3)

Gelasinospora sp. (Type HdV-1) (Figure 7, 4)

Microthyriaceae s.l. (Figure 7, 20)

cf. *Schizothecium* sp. (Figure 7, 1)

Sordaria-type (*fide* van Geel et al., 2003) (Type HdV-55A) (Figure 7, 8)

Sphaerodes sp. (*fide* Borel et al. 2001) (Figure 7, 5)

cf. *Sphaerodes* sp. (Figure 7, 6)

Sporormiella-type (*fide* van Geel et al., 2003) (Type HdV-113) (Figure 7, 9)

Type 810 cf. *Byssothecium alpesense* (Tóth) Boise, 1989 (*fide* Mauquoy et al., 2004)
(Figure 7, 10)

Mitosporic fungi

Alternaria sp. (Figure 7, 14)

Arthrimum puccinioides Kunze & Schmidt, 1823 (Figure 7, 13)

Dictyosporium sp. (Figure 7, 15)

Endophragma sp. (Figure 7, 16)

Tetraploa aristata Berkeley & Broome, 1850 (Type HdV-89) (Figure 7, 17)

Incertae sedis

Type HdV-181 (*fide* van Geel et al., 1983) (Figure 7, 12)

Type HdV-1033 (*fide* van Geel et al., 2011) (Figure 7, 11)

Acknowledgements

This paper was funded by grants PICT 2012-0628 (to Andrea Coronato) and PIP-CONICET 2014-0323 (to Ana Borromei). The authors thank to Juan Federico Ponce and Diego Quiroga (CADIC-CONICET) for their assistance during the fieldwork. Also thanks are to Ignacio Magneres (CADIC-CONICET) for textural determinations by means of a laser grain-size particle analyzer. Our thanks are also extended to Maarten Blaauw (School of Natural and Built Environment, Queen's University Belfast, UK) and Pablo Esteban Díaz (INGEOSUR-CONICET, Bahía Blanca, Argentina) for providing assistance with the management of the chronologies. Last we thank four anonymous reviewers who helped to improve substantially the manuscript.

References

- Cingolani, A.M., 1999. Efectos de 100 años de pastoreo ovino sobre la vegetación y suelos del norte de Tierra del Fuego. PhD. Thesis. Unpublished. Facultad de Ciencias Exactas y Naturales, Universidad de Buenos Aires, Buenos Aires, pp. 213.
- Oliva, G., 1996. Biología de poblaciones de *Festuca gracillima*. PhD. Thesis. Unpublished. Facultad de Ciencias Exactas y Naturales. Universidad de Buenos Aires, Buenos Aires, pp. 121.
- Quiroga, D., 2018. La incidencia de los agentes naturales y antropogénicos en la evolución geomorfológica de la región Río Chico-Río Grande, Tierra del Fuego. PhD. Thesis. Unpublished. Universidad Nacional del Sur, Bahía Blanca, pp. 215.
- Rauber, R.B., 2011. Invasión de *Hieracium pilosella* L. en pastizales de Tierra del Fuego. PhD. Thesis. Unpublished. Facultad de Ciencias Exactas y Naturales, Universidad de Buenos Aires, Buenos Aires, pp. 101.

- Sánchez, R.M., 2011. Estudio Sistemático de Micromicetes de la Región Andino-patagónica. PhD. Thesis. Unpublished. Universidad Nacional del Sur, Bahía Blanca, pp. 238.
- Adam, D.P., Merhinger, P.J., 1975. Modern pollen surface sample: analysis of subsamples. *J. Res. U.S. Geol. Surv.* 3, 733–736.
- Almeida-Lenero, L., Hooghiemstra, H., Cleef, A.M., van Geel, B., 2005. Holocene climatic and environmental change from pollen records of lakes Zempoala and Quila, central Mexican highlands. *Rev. Palaeobot. Palynol.* 136, 63–92.
- Baker, A.G., Bhagwat, S.A., Willis, K.J., 2013. Do dung tungal spores make a good proxy for past distribution of large herbivores? *Quat. Sci. Rev.* 62, 21–31.
- Berman, A.L., Silvestri, G., Compagnucci, R., 2012. Eastern Patagonia Seasonal Precipitation: Influence of Southern Hemisphere Circulation and Links with Subtropical South American Precipitation. *J. Clin.* 25, 6781–6795.
- Birks, H.J., Birks, H.H., 1980. Quaternary palaeoecology. Arnold Publishers Limited, London, pp. 289.
- Blaauw, M., Christen, J.A., 2011. Flexible paleoclimate age-depth models using an autoregressive gamma process. *Bayesian Anal.* 6, 457–474.
- Borel, C.M., Biancinotti, M.V., Quattrocchio, M., 2001. Palinomorfos fúngicos en sedimentos del Pleistoceno-Holoceno del Valle Medio del Arroyo Chasicó, Provincia de Buenos Aires. *Polen* 11, 21–37.
- Borromei, A.M., Coronato, A., Quattrocchio, M., Rabassa, J., Grill, S., Roig, C., 2007. Late Pleistocene-Holocene environments in Valle Carbajal, Tierra del Fuego, Argentina. *J. South Am. Earth Sci.* 23, 321–335.
- Borromei, A.M., Coronato, A., Franzén, L.G., Ponce, J.F., López Sáez, J.A., Maidana, N., Rabassa, J., Candel, M.A., 2010. Multiproxy record of Holocene

paleoenvironmental change, Tierra del Fuego, Argentina. *Palaeogeogr. Palaeoclimatol. Palaeoecol.* 286, 1–16.

Borromei, A.M., Ponce, J.F., Coronato, A., Candel, M.S., Olivera, D., Okuda, M., 2014. Reconstrucción de la vegetación posglacial y su relación con el ascenso relativo del nivel del mar en el extremo este del canal Beagle, Tierra del Fuego. *Andean Geol.* 41 (2), 362–379.

Borromei, A.M., Musotto, L.L., Coronato, A., Ponce, J.F., Pontevedra-Pombal, X., 2016. Postglacial vegetation and climate changes inferred from a peat pollen record in the Río Pipo Valley, southern Tierra del Fuego, in: Martínez, M., Olivera, D. (Eds.), *Palinología del Meso-Cenozoico de Argentina*. E-Publishing Asoc. Paleont. Arg. 16 (2), pp. 168–183.

Borromei, A.M., Candel, M.S., Musotto, L.L., Cusminsky, G., Martínez, M.A., Coviaga, C.A., Ponce, J.F., Coronato, A., 2018. Late Holocene wet/dry intervals from Fuegian steppe at Laguna Carmen, southern Argentina, based on a multiproxy record. *Palaeogeogr. Palaeoclimat. Palaeoecol.* 499, 56–71.

Campbell, I.D., 1999. Quaternary pollen taphonomy: examples of differential redeposition and differential preservation. *Palaeogeogr. Palaeoclimat. Palaeoecol.* 149, 245–256.

Candel, M.S., Díaz, P.E., Borromei, A.M., Fernández, M., Montes, A. Santiago, F.C., 2020. Multiproxy analysis of a Lateglacial-Holocene sedimentary section in the Fuegian steppe (northern Tierra del Fuego, Argentina): Implications for coastal landscape evolution in relation to climatic variability and sea-level fluctuations. *Palaeogeogr. Palaeoclimat. Palaeoecol.* 557, 109941. <https://doi.org/10.1016/j.palaeo.2020.109941>.

Caseldine, C.J., Matthews, J.A., 1985. ^{14}C Dating of Palaeosols, Pollen Analysis and Landscape Change: Studies from the Low- and Mid-Alpine Belts of Southern Norway,

in: Boardman, J. (Ed.), Soils and Quaternary Landscape Evolution. John Wiley & Sons Ltd., New York, pp. 87–116.

Catt, J.A., 1990. Paleopedology Manual, Quaternary International 6. Pergamon Press Oxford, 95 pp.

Cavagnaro, R.A., Pero, E., Dudinszky, N., Golluscio, R.A., Grimoldi, A.A., 2019. Under pressure from above: Overgrazing decreases mycorrhizal colonization of both preferred and unpreferred grasses in the Patagonian steppe. *Fungal Ecol.* 40, 92–97.

Cipriotti, P.A., Collantes, M.B., Escartín, C., Cabeza, S., Ramirez, R.B., Braun, K., 2014. Experiencias de largo plazo para el manejo de una hierba invasora de pastizales: El caso de *Hieracium pilosella* L. en la Estepa Fueguina. *Ecol. Austral* 24, 135–144.

Collantes, M.B., Anchorena, J., Ontivero, J., Cingolani, M., 1987. Las comunidades edáficas de la región magallánica de Tierra del Fuego. Actas XIII Reunión Argentina de Ecología. Bahía Blanca, Argentina.

Collantes, M.B., Anchorena, J., Cingolani, A.M., 1999. The steppes of Tierra del Fuego: floristic and growthform patterns controlled by soil fertility and moisture. *Plant Ecol.* 140, 61–75.

Collantes, M.B., Braun, K., Escartín, C., Cingolani, A.M., Anchorena, J., 2005. Patrones de cambio de la vegetación de la estepa fueguina en relación al pastoreo, in: Oesterheld, M., Aguiar, M., Ghersa, C., Paruelo, J. (Eds.), La heterogeneidad de la vegetación de los agroecosistemas. Editorial de la Facultad de Agronomía, Universidad de Buenos Aires, Buenos Aires, Argentina, pp. 235–251.

Collantes, M.B., Escartín, C., Braun, K., Cingolani, A., Anchorena, J., 2013. Grazing and grazing exclusion along a resource gradient in Magellanic meadows of Tierra del Fuego. *Rangeland Ecol. Manage* 66, 688–699.

- Coronato, A., Coronato, F., Mazzoni, E., Vázquez, M., 2008. Physical geography of Patagonia and Tierra del Fuego, in: Rabassa, J. (Ed.), Late Cenozoic of Patagonia and Tierra del Fuego. Developments in Quaternary Sciences. Elsevier, Amsterdam pp. 13–55.
- Coronato, A., Fanning, P., Salemme, M., Oría, J., Pickard, J., Ponce, J.F., 2011. Aeolian sequence and the archaeological record in the Fuegian steppe, Argentina. *Quat. Int.* 245, 122–135.
- Coronato, A., Salemme, M., Oría, J., Mari, F., López, R., 2021. Perched dunes in the Fuegian steppe, Southern Argentina: Archeological reservoirs of Holocene information, in: Collantes, M.M., Perucca, L., Niz, A., Rabassa, J. (Eds.), *Advances in Geomorphology and Quaternary Studies in Argentina*. Springer Earth System Sciences. Springer, Cham, pp. 58–91.
- Crosta, S., Villarreal, L., Coronato, A., 2014. Formación de cristales de hialita en Laguna Escondida, norte de Tierra del Fuego. Reunión Argentina de Geoquímica de la Superficie. *Actas de Resúmenes Extendidos III*, pp. 57–61. Mar del Plata, Argentina.
- Davies, B.E., 1974. Loss-on-ignition as an estimate of soil organic matter 1. *Soil Sci. Soc. Am. J.* 38 (1), 150–151.
- De Linares, C., Belmonte, J., Canela, M., Díaz de la Guardia, C., Alba-Sanchez, F., Sabariego, S., Alonso-Pérez, S., 2010. Dispersal patterns of *Alternaria* conidia in Spain. *Agric. For. Meteorol.* 150, 1491–1500.
- Echeverría, M.E., Bamonte, F.P., Marcos, M.A., Sottile, G.D., Mancini, M.V., 2017. Palaeohydric balance variations in eastern Andean environments in southern Patagonia (48°–52.5° S): major trends and forcings during the last ca. 8000 cal yrs BP. *Rev. Palaeobot. Palynol.* 246, 242–250.

- Ellis, M.B., 1971. Dematiaceous Hyphomycetes. Commonwealth Mycological Institute, Kew, England, 608 pp.
- Favier Dubois, C., 2003. Late Holocene climatic fluctuations and soil genesis in southern Patagonia: effects on the archaeological record. *J. Archaeol. Sci.* 30, 1657–1664.
- Favier-Dubois, C., 2007. Soil genesis related to medieval climatic fluctuations in southern Patagonia and Tierra del Fuego (Argentina): Chronological and paleoclimatic considerations. *Quat. Int.* 162–163, 158–165.
- Fenwick, I.M., 1985. Paleosols: problems of recognition and interpretation, in: Boardman, J. (Ed.), *Soils and Quaternary Landscape Evolution*. John Wiley & Sons Ltd., New York, pp. 3–22.
- Fernández, M., Maidana, N.I., Ponce, J.F., Oja, J., Salemme, M., Coronato, A., 2018. Palaeoenvironmental conditions for human settlement at the Fuegian steppe (Argentina) based on diatom analysis. Lake Arturo as a case study. *J. Archaeol. Sci. Reports* 18, 775–781.
- Fernández, M., Ponce, J.F., Pamón Mercau, J., Coronato, A., Laprida, C., Maidana, N., Quiroga, D., Magneres, F., 2020a. Paleolimnological response to climate variability during Late Glacial and Holocene times: a record from Lake Arturo, located in the Fuegian steppe, southern Argentina. *Palaeogeogr. Palaeoclimatol. Palaeoecol.* 550, 109737. <https://doi.org/10.1016/j.palaeo.2020.109737>.
- Fernández, M., Ponce, J.F., Zangrando, F.J., Borromei, A.M., Musotto, L.L., Alunni, D., Vázquez, M., 2020b. Relationships between terrestrial animal exploitation, marine hunter-gatherers and palaeoenvironmental conditions during the Middle-Late Holocene in the Beagle Channel region (Tierra del Fuego). *Quat. Int.* 549, 208–217.

- Frazer, H., Prieto, A.R., Carbonella, J.C., 2020. Modern pollen source and spatial distribution from surface, lake sediments in the southwestern Pampa grasslands, Argentina: Implications to interpret Holocene pollen records. *Rev. Palaeobot. Palynol.* 277, 104207. <https://doi.org/10.1016/j.revpalbo.2020.104207>.
- García Massini, J.L., Zamalao, M. del C., Romero, E.J., 2004. Fungal fruiting bodies in the Cullen Formation (Miocene) in Tierra del Fuego, Argentina. *Ameghiniana* 41 (1), 83–90.
- Garreaud, R., Lopez, P., Minvielle, M., Rojas, M., 2013. Large-scale control on the Patagonian climate. *J. Clim.* 26, 215–230.
- van Geel, B., Hallewas, D.P., Pals, J.P., 1983. A late Holocene deposit under the Westfriese Zeedijk near Enkhuizen (Prov. of Noord-Holland, The Netherlands): palaeoecological and archaeological aspects. *Rev. Palaeobot. Palynol.* 38, 269–335.
- van Geel, B., Buurman, J., Brinkkemper, O., Schelvis, J., Aptroot, A., Reenen, G., Hakbijl, T., 2003. Environmental reconstruction of a Roman Period settlement site in Uitgeest (The Netherlands), with special reference to coprophilous fungi. *J. Archaeol. Sci.* 30, 873–883.
- van Geel, B., Gelorini, V., Ujvaruu, A., Aptroot, A., Rucina, S., Marchant, R., Sinnighe Damsté, J.S., Verschuren, D., 2011. Diversity and ecology of tropical African fungal spores from a 25,000-year palaeoenvironmental record in southeastern Kenya. *Rev. Palaeobot. Palynol.* 164, 174–190.
- Greif, M.D., Currah, R.S., 2007. Patterns in the occurrence of saprophytic fungi carried by arthropods caught in traps baited with rotted wood and dung. *Mycologia* 99 (1), 7–19.
- Grimm, E., 2012. Tilia and TGView 2.0.2. Software. Illinois State Museum. Research and Collection Center, Springfield, USA.

- Hartge, K.H., 1994. Soil structure, its development and its implications for properties and processes in soils -a synopsis based on recent research in Germany. *J. Plant. Nutr. Soil Sci.* 157 (3), 159–164.
- Heusser, C.J., 1989. Late Quaternary vegetation and climate of southern Tierra del Fuego. *Quat. Res.* 31, 396–406.
- Heusser, C.J., 2003. Ice Age Southern Andes—A chronicle of paleoecological events. (Developments in Quaternary Science 3), first ed. Elsevier, Amsterdam, 240 pp.
- Heusser, C.J., Heusser, L.E., Hauser, A., 1989-1990. A 12,000 yr B.P. tephra layer at Bahía Inútil (Tierra del Fuego, Chile). *An. Inst. Patagor.* 13, 39–49.
- Hoang, T.K., Probst, A., Orange D., Gilbert, F., Fléger, A., Kallerhoff, J., Laurent, F., Bassil, B., Duong, T.T., Gerino, M., 2018. Bioturbation effects on bioaccumulation of cadmium in the wetland plant *Typha latifolia*: A nature-based experiment. *Sci. Total Environ.* 618, 1284–1297.
- Hogg, A.G., Heaton, T.J., Hua, Q., Palmer, J.G., Turney, C.S.M., Southon, J., Bayliss, A., Blackwell, P.G., Boswijk, G., Bronk Ramsey, C., Pearson, C., Petchey, F., Reimer, P.J., Reimer, R.W., Wacker, L., 2020. SHCal20 Southern Hemisphere calibration, 0–55,000 years cal BP. *Radiocarbon* 62. doi: 10.1017/RDC.2020.59
- Kilian, R., Lamy, F., 2012. A review of Glacial and Holocene paleoclimate records from southernmost Patagonia (49–55° S). *Quat. Sci. Rev.* 53, 1–23.
- Kristensen, E., Penha-Lopes, G., Delefosse, M., Valdemarsen, T., Quintana, C.O., Banta, G.T., 2012. What is bioturbation? The need for a precise definition for fauna in aquatic sciences. *Mar. Ecol. Prog. Ser.* 446, 285–302.
- Laprida, C., Orgeira, M.J., Fernández, M., Tófaló, R., Ramón Mercau, J., Silvestri, G.E., Berman, A.L., García Chaporí, N., Plastani, M.S., Alonso, S., 2021. The role of

Southern Hemispheric Westerlies for Holocene hydroclimatic changes in the steppe of Tierra del Fuego (Argentina). *Quat. Int.* 571, 11–25.

Limaye, R.B., Kumaran, K.P.N., Nair, K.M., Padmalal, D., 2007. Non-pollen palynomorphs as potential palaeoenvironmental indicators in the Late Quaternary sediments of the west coast of India. *Curr. Sci.* 92 (10), 1370–1382.

Lukens, W.E., Nordt, L.C, Stinchcomb, G.E., Driese, S.G., Tubbs, J.D., 2018. Reconstructing pH of Paleosols Using Geochemical Proxies. *J. Geol.* 126, 427–449.

Mansilla, C.A., McCulloch, R.D., Morello, F., 2016. Palaeoenvironmental change in southern Patagonia during the Lateglacial and Holocene: implications for forest refugia and climate reconstructions. *Palaeogeogr. Palaeoclimatol. Palaeoecol.* 447, 1–11.

Mansilla, C.A., McCulloch, R.D., Morello, F., 2018. The vulnerability of the *Nothofagus* forest-steppe ecotone to climate change: Palaeoecological evidence from Tierra del Fuego (~53°S). *Palaeogeogr. Palaeoclimatol. Palaeoecol.* 508, 59–70.

Markgraf, V., 1993. Paleoenvironments and paleoclimates in Tierra del Fuego and southernmost Patagonia, South America. *Palaeogeogr. Palaeoclimatol. Palaeoecol.* 102, 53–68.

Markgraf, V., Huber, U.M., 2010. Late and postglacial vegetation and fire history in Southern Patagonia and Tierra del Fuego. *Palaeogeogr. Palaeoclimatol. Palaeoecol.* 297, 351–366.

Matthews, J.A., 1985. Radiocarbon dating of surface and buried soil: principles, problems and prospects. In: Richards, K., Arlett, R., Ellis, S. (Eds.), *Geomorphology and Soils*. Allen and Unwin, London, pp. 269–288.

Mauquoy, D., Blaauw, M., van Geel, B., Borromei, A., Quattrocchio, M., Chambers, F., Possnert, G., 2004. Late-Holocene climatic changes in Tierra del Fuego based on multi-proxy analyses of peat deposits. *Quat. Res.* 61, 148–158.

- McClung de Tapia, E., Domínguez Rubio, I., Gama Castro, J., Solleiro, E., Sedov, S., 2005. Radiocarbon dates from soil profiles in the Teotihuacán Valley, Mexico: Indicators of geomorphological processes. *Radiocarbon* 47(1), 159–175.
- Mendoza, R.E., Cabello, M., Anchorena, J., García, I., Marbán, L., 2011. Soil parameters and host plants associated with arbuscular mycorrhizae in the grazed Magellanic steppe of Tierra del Fuego. *Agric. Ecosyst. Environ.* 140, 411–418.
- Miola, A., 2012. Tools for Non-Pollen Palynomorphs (NPPs) analysis: A list of Quaternary NPP types and reference literature in English language (1972–2011). *Rev. Palaeobot. Palynol.* 186, 142–161.
- Montes, A., Santiago, F., Salemme, M., López, R., 2020. Late Pleistocene and Holocene geomorphologic evolution of Laguna Las Vueltas area, Tierra del Fuego (Argentina). *Andean Geol.* 47 (1), 61–76.
- Moore, D.M., 1983. *Flora of Tierra del Fuego*, first ed. Nelson, Oswestry.
- Munsell, A.H., 1973. *Munsell soil colour charts*. Kollmorgen Corporation, Baltimore.
- Musotto, L.L., Bianchinotti, M.V., Borromei, A.M., 2013. Inferencias paleoecológicas a partir del análisis de microfósiles fúngicos en una turbera pleistoceno-holocena de Tierra del Fuego (Argentina). *Rev. Mus. Arg. Cienc. Nat.* 15 (1), 89–98.
- Musotto, L.L., Bianchinotti, M.V., Borromei, A.M., 2012. Pollen and fungal remains as environmental indicators in surface sediments of Isla Grande de Tierra del Fuego, southernmost Patagonia. *Palynology* 36, 162–179.
- Musotto, L.L., Borromei, A.M., Candel, M.S., Mehl, A., Bianchinotti, M.V., Coronato, A., Ponce, J.F., 2018. Condiciones ambientales durante el Holoceno medio-tardío registradas en paleosuelos de Laguna Arturo, norte de Tierra del Fuego, en base al análisis palinológico, in: VII Congreso Argentino de Geomorfología y Cuaternario.

Naturalia Patagónica. Universidad Nacional de la Patagonia San Juan Bosco Vol. 10, 70–71. Puerto Madryn, Argentina.

Musotto, L.L., Borrromei, A.M., Coronato, A., Menounos, B., Osborn, G., Marr, R., 2016. Late Pleistocene and Holocene palaeoenvironmental changes in central Tierra del Fuego (~54°S) inferred from pollen analysis. *Veg. Hist. Archaeobot.* 25, 117–130.

Musotto, L.L., Borrromei, A.M., Bianchinotti, M.V., Coronato, A., 2017a. Late Quaternary palaeoenvironmental reconstruction of central Tierra del Fuego (Argentina) based on pollen and fungi. *Quat. Int.* 442, 13–25.

Musotto, L.L., Borrromei, A.M., Bianchinotti, M.V., Coronato, A., Menounos, B., Osborn, G., Marr, R., 2017b. Postglacial environment in the southern coast of Lago Fagnano, central Tierra del Fuego, Argentina, based on pollen and fungal microfossils analyses. *Rev. Palaeobot. Palynol.* 238, 43–54.

O’Keefe, J.M.K., Nuñez Otaño, N.B., Bianchinotti, M.V., 2021. Nomenclature: how do we designate NPP taxa?. In: Marret, F., O’Keefe, J., Osterloff, P., Pound, M. and Shumilovskikh, L. (Eds). *Applications of Non-Pollen Palynomorphs: from Palaeoenvironmental Reconstructions to Biostratigraphy*. Geological Society, London, Special Publications, 511, <https://doi.org/10.1144/SP511-2020-119>.

Orgeira, M.J., Vázquez, C.A., Coronato, A., Ponce, J.F., Moreto, A., Osterrieth, M., Egli, R., Onorato, R., 2012. Magnetic properties of Holocene edaphized silty eolian sediments from Tierra del Fuego (Argentina). *Rev. Soc. Geol. Esp.* 25 (1–2), 45–56.

Oría, J., 2014. Tierra adentro. Distribuciones artefactuales y movilidad en la estepa fueguina. In: Oría, J., Tivoli, A. (Eds.). *Cazadores de mar y tierra. Estudios recientes en arqueología fueguina*. Editora Cultural Tierra del Fuego, Ushuaia, Argentina, pp. 289–312.

- Oría, J., Salemme, M., 2016. Visibilidad y preservación en Laguna Arturo, norte de Tierra del Fuego (Argentina). Un análisis geoarqueológico. *Intersecciones en Antropología, La Geoarqueología en la Argentina, aportes y avances, Volumen Especial 4*, 89–100.
- Oría, J., Salemme, M., Vázquez, M., 2016. Site formation processes in relation to surface bone assemblages in the Fuegian steppe (Tierra del Fuego, Argentina). *Archaeol. Anthropol. Sci.* 8, 291–304.
- Page, A.L., 1982. *Methods of soil analysis. Part 2. Chemical and microbiological properties*, second ed. Agronomy no. 9, American Society of Agronomy and Soil Science Society of America, Madison, Wisconsin, USA, 1142 pp.
- Paruelo, J.M., Beltrán, A., Jobbágy, E., Sala, O.F., Collucio, R.A., 1998. The climate of Patagonia: general patterns and controls on biotic processes. *Ecol. Austral* 8, 85–101.
- Posse, G., Anchorena, J., Collantes, M.B., 2000. Spatial micro-patterns in the steppe of Tierra del Fuego induced by sheep grazing. *J. Veg. Sci.* 11, 43–50.
- Saccardo, P.A., 1886. *Sylloge Fungorum* 4, 1–807.
- Schaefer, C.E.R., Dalrymple, J., 1996. Pedogenesis and relict properties of soils with columnar structure from Kerima, north Amazonia. *Geoderma* 71, 1–17.
- Smith, S.E., Read, D.J., 2008. *Mycorrhizal Symbiosis*, third ed. Academic Press, New York, 800 pp.
- Soil Survey Staff, 1999. *Keys to soil taxonomy*, eighth ed. USDA Natural Resource Conservation Service, Washington, DC.
- Stanley, E.A., 1966. The problem of reworked pollen and spores in marine sediments. *Mar. Geol.* 4, 397–408.
- Stern, C.R., 2008. Holocene tephrochronology record of large explosive eruptions in the southernmost Patagonian Andes. *Bull. Volcanol.* 70, 435–454.

- Stockmarr, J., 1971. Tablets with spores used in absolute pollen analysis. *Pollen Spores* 13, 615–621.
- Stuiver, M., Reimer, P.J., Reimer, R.W., 2021. CALIB 8.2. [WWW program] <http://calib.org/calib/> (accessed 2 September 2021).
- Tanaka, K., Hirayama, K., Yonezawa, H., Hatakeyama, S., Harada, Y., Sano, T., Shirouzu, T., Hosoya, T., 2009. Molecular taxonomy of bambusicolous fungi: Tetraplosphaeriaceae, a new pleosporalean family with *Tetraploa*-like anamorphs. *Stud. Mycol.* 64, 175–209.
- Trivi de Mandri, M.E., Burry, L.S., D'Antoni, H.L., 2006. Dispersión-depositación del polen actual en Tierra del Fuego, Argentina. *Rev. Mex. Biodivers.* 77, 89–95.
- Velázquez, N.J., Burry, L.S., 2012. Palynological analysis of Lama guanicoe modern feces and its importance for the study of coprolites from Patagonia, Argentina. *Rev. Palaeobot. Palynol.* 184, 14–23.
- Vilanova, I., Moreno, P.I., Miranda, C.G., Villa-Martínez, R.P., 2019. The last glacial termination in the Coyhaique sector of central Patagonia. *Quat. Sci. Rev.* 224, 105976. <https://doi.org/10.1016/j.quascirev.2019.105976>.
- Villarreal, M.L., Coronato, A., 2017. Characteristics and nature of pans in the semiarid temperate-cold steppe of Tierra del Fuego, in: Rabassa, J. (Ed.) *Advances in Geomorphology and Quaternary Studies in Argentina*, Springer Earth System Sciences. Springer, Cham, pp. 203–224.
- Villarreal, M.L., Coronato, A., Mazzoni, E., López, R., 2014. Mantos eólicos y lagunas semipermanentes de la Estepa Fueguina (53°S), Argentina. *Rev. Soc. Geol. Esp.* 27 (2), 81–96.
- Waldmann, N., Borromei, A.M., Recasens, C., Olivera, D., Martínez, M.A., Maidana, N.I., Ariztegui, D., Austin Jr., J.A., Anselmetti, F.S., Moy, C.M., 2014. Integrated

reconstruction of Holocene millennial-scale environmental changes in Tierra del Fuego, southernmost South America. *Palaeogeogr. Palaeoclimatol. Palaeoecol.* 399, 294–309.

Walker, M., 2005. *Quaternary Dating Methods*. John Wiley and Sons Ltd., Chichester, England, 286 pp.

Wang, Y., Amundson, R., Trumbore, S., 1996. Radiocarbon dating of soil organic matter. *Quat. Res.* 45, 282–288.

Wearn, J.A., Gange, A.C., 2007. Above-ground herbivory causes rapid and sustained changes in mycorrhizal colonization of grasses. *Oecologia* 153, 959–971.

Wille, M., Maidana, N.I., Schäbitz, F., Fey, M., Haberzettl, T., Janssen, S., Lücke, A., Mayr, C., Ohlendorf, C., Schleser, G.H., Zolitschka, B., 2007. Vegetation and climate dynamics in southern South America: The microfossil record of Laguna Potrok Aike, Santa Cruz, Argentina. *Rev. Palaeobot. Palynol.* 146, 234–246.

Woudenberg, J.H.C., Groenewald, J.Z., Binder, M., Crous, P.W., 2013. *Alternaria* redefined. *Stud. Mycol.* 75, 171–212.

Zolitschka, B., Fey, M., Janssen, S., Maidana, Nora I., Mayr, C., Wulf, S., Haberzettl, T., Corbella, H., Lücke, A., Ohlendorf, C., Schäbitz, F., 2019. Southern Hemispheric Westerlies control sedimentary processes of Laguna Azul (south-eastern Patagonia, Argentina). *Holocene* 29 (3), 403–420.

Table and figure captions

Table 1. Radiocarbon dates and calibrated ages obtained from organic matter deposited in palaeosol levels at Laguna Arturo, Tierra del Fuego, Argentina.

Table 2. Vegetation and environment at sampling sites in the Fuegian steppe. Note: the samples have been arranged according to their occurrence in physio-floristic types in the

tussock steppe of *Festuca gracillima*. Surface samples MS 1 to MS 13 have already been published in Musotto et al. (2012).

Figure 1. (A) Satellite image of the Fuegian Archipelago showing the location of Laguna Arturo (yellow arrow) and the other sites cited in the text (white circles), and of the previously published surface samples (red circles) (image downloaded from SAS Planet, free version). (B) Aerial photograph of Laguna Arturo showing the location of the new sampled sites and archaeological sites (taken from Google Earth, free version) (C) Present vegetation map of northern Isla Grande de Tierra del Fuego with the mean annual precipitation isohyets (modified from Collantes et al., 1999). The location of studied paleosols in the Arturo dune (red circle), and the meteorological station (green star) are shown as well. (D) Complete sequence of the eolian–paleosols from the top. Eolian erosion and deposition occur on top of the sequence where steppe vegetation can be observed.

Figure 2. (A) Stratigraphy of the eolian sedimentary profile of the Arturo dune (modified from Coronato et al., 2011). Studied paleosols are marked by red star. (B) Details of the three uppermost paleosols (Ps6, Ps7 and Ps8) developed at the Arturo dune and analyzed in this contribution. Horizonation and thickness are indicated along with a general view of each paleosol.

Figure 3. Surface pollen and fungal frequency diagram (%) showing vegetation units from Isla Grande de Tierra del Fuego (modified from Musotto et al., 2012). Sample numbers are presented as in the original published works. Unpublished samples from Laguna Arturo area are showed with black circles.

Figure 4. Fossil pollen and fungal frequency (%) and concentration (palynomorphs gram^{-1}) diagram from Paleosol 6; shaded parts of curves indicate an exaggeration of 10 \times .

Figure 5. Fossil pollen and fungal frequency (%) and concentration (palynomorphs gram⁻¹) diagram from Paleosol 7; shaded parts of curves indicate an exaggeration of 10×.

Figure 6. Fossil pollen and fungal frequency (%) and concentration (palynomorphs gram⁻¹) diagram from Paleosol 8; shaded parts of curves indicate an exaggeration of 10×.

Figure 7. Fungal remains found in modern surface steppe samples and fossil samples from Ps6, Ps7 and Ps8. Each photograph indicates the sample number, and England Finder coordinates. 1. cf. *Schizothecium* sp., UNSP PDA4620: X39/2; 2. *Coniochaeta* cf. *lignaria* (HdV-172), UNSP PDA4585: T57/4; 3. *Arthrinium puccinioides*, UNSP MS4631: D34/1; 4. cf. *Delitschia pachyspora*, UNSP PDA4623: V39/1; 5. *Gelasinospora* sp. (HdV-1), UNSP PDA4622: R37; 6. *Sphaerodes* sp. (*fide* Borel et al., 2001), UNSP PDA4625: X35; 7. *Cercophora*-type (HdV-112), UNSP PDA4584: Y62/4; 8. *Sordaria*-type (*fide* van Geel et al., 2003) (HdV-55A), UNSP MS4599: V75/1; 9. *Sporormiella*-type (*fide* van Geel et al., 2003) (HdV-113), UNSP PDA4623: M33/3; 10. Type 810 cf. *Rhizothecium alpestre* (*fide* Mauquoy et al., 2004), UNSP PDA4620: R29/3; 11. cf. *Sphaerodes* sp., UNSP PDA4594: T69/3; 12. Type HdV-181, UNSP PDA4584: Y62/4; 13. Type HdV-1033 (*fide* van Geel et al., 2011), UNSP PDA4594: H73/2; 14. *Alternaria* sp., UNSP PDA4589: T46; 15. *Dictyosporium* sp., UNSP PDA4584: U61; 16. *Endophragma* sp., UNSP PDA4592: Y54; 17. *Tetraploa aristata*, UNSP MS4596b: W25; 18. *Glomus* sp. (HdV-1103), UNSP PDA4594: R44/4; 19. cf. *Acaulospora* sp., UNSP PDA4584: V58; 20-21. Entire reproductive bodies of Microthyriaceae s.l. (20: UNSP PDA4626: E22/3; 21: UNSP PDA4591: L56/4); 22. cf.

Cryptendoxyla hypophloia, UNSP PDA4589: Y66/4. Scale bar is 5 μm except in photos 4 and 16–22 where the scale bar is 10 μm .

Journal Pre-proof

Sedimentary units	Laboratory code	Sample depth (cm)	Uncalibrated age (^{14}C yr BP)	Calibrated years BP (median probability)	1 σ range	2 σ range
Palaeosol 8	D-AMS 019982 ^a	0–2	1538 \pm 41	1377	1346 - 1411	1305 - 1432
Palaeosol 8	D-AMS 019981 ^a	45–47	2406 \pm 52	2415	2332 - 2493	2306 - 2540
Palaeosol 7	AA108182 ^b	0–2	1752 \pm 22	1620	1657 - 1695	1561 - 1633
Palaeosol 7	AA108181 ^b	50–52	2902 \pm 24	2987	2939 - 3008	2872 - 3076
Palaeosol 6	AA108180 ^b	0–2	4424 \pm 26	4948	4873 - 4976	4854 - 5051
Palaeosol 6	AA108179 ^b	25–27	5066 \pm 27	5799	5808 - 5892	5702 - 5897

^aDirectAMS Radiocarbon Dating Service.

^bNSF Arizona AMS Facility.

Table 1

Sample code	Vegetation and Environment	Physio-floristic types in the tussock steppe of <i>Festuca gracillima</i>
MS 21	Overgrazing site in the playa surrounding the lake with cushion plants and grasses	S1 Steppe
MS 19	Overgrazing site close to a shearing pen with cushion plants, shrubs and grasses	
MS 15	Grazing hill without tussock grasses	S2 Steppe
MS 17	Grazing site in the playa surrounding the lake with grass vegetation	
MS 20	Grazing hill with tussock grasses	
MS 16	Hill with tussock grasses	S3 Steppe
MS 18	Hill with tussock grasses	
MS 9	Herbaceous communities (Musotto et al., 2012)	
MS 10	Sedge and herb communities (Musotto et al., 2012)	
MS 11	Shrub, herb and sedge communities (Musotto et al., 2012)	

Table 2

Declaration of interests

The authors declare that they have no known competing financial interests or personal relationships that could have appeared to influence the work reported in this paper.

The authors declare the following financial interests/personal relationships which may be considered as potential competing interests:

- Paleoenvironmental reconstruction from paleosols in the Fuegian steppe during the mid-to late Holocene.
- Paleosols development is associated with periods of landscape stability
- Palynological and pedological data provide evidences for the variations in moisture availability at the Arturo perched dune.

Journal Pre-proof